COBEM 2021 26th International Congress of Mechanical Engineering
November 22-26, 2021, Virtual Congress, Brazil
ABCM Associação Brasileira de Engenharia e Ciências Mecânicas

COB-2021-0608
EXPLORATORY EVALUATION OF THE T_0 REFERENCE TEMPERATURE FOR A HIGH STRENGTH MARTENSITIC STEEL USING THE MASTER CURVE APPROACH

Vinicius Mota da Cruz Gomes
Vitor Scarabeli Barbosa
Claudio Ruggieri
Polytechnic School of Engineering, University of São Paulo, Brazil
vinimcg@usp.br, scarabeli@usp.br, claudio.ruggieri@usp.br

Abstract. *This work addresses an experimental investigation of the brittle fracture behavior for a high strength martensitic steel using conventional three-point bend specimens. The purpose of this work is to assess the applicability of the Master Curve methodology in providing a reliable estimate of the reference temperature (T_0) derived from fracture toughness data sets measured in the ductile-to-brittle transition region (DBT) of a direct-quenched low alloy martensitic steel. Fracture toughness tests conducted at different temperatures in the DBT region provide the fracture toughness data in terms of the J-integral at instability point, J_c. The measured distributions of fracture toughness values showed a relatively smaller scatter compared to the theoretical scatter specified by ASTM E1921 standard and provided mean curves of fracture toughness vs. temperature that slightly deviate from the theoretical master curve. Even though the toughness-temperature behavior and scatter were shown to deviate from the ASTM E1921 predictions, the use of Master Curve in its standard formulation still provides a good description of the fracture toughness dependence with temperature for the tested material.*

Keywords: *master curve, reference temperature, fracture toughness, ductile-to-brittle transition temperature, direct-quenched martensitic steel.*

1. INTRODUCTION

Reliable structural integrity assessments are of utmost importance in fitness-forpurpose (FFP) analysis or engineering critical assessment (ECA) methods of engineering structural components containing crack-like flaws to ensure acceptable safety levels during normal and emergency operating conditions. These methods such as, for example, API 579 (API RP-579-1 / ASME FFS-1, 2016) and BS 7910 (BS 7910, 2019), among others, rely on a detailed knowledge of the relationships between tolerable crack sizes and applied loading as measured by the linear elastic stress intensity factor, K, or the elastic-plastic parameter defined by the J-integral and its corresponding value of the Crack Tip Opening Displacement, (CTOD or δ). In particular, the unstable fracture by transgranular cleavage represents one of the most serious failure modes of components and equipment made of ferritic steels operating in the ductile-to-brittle transition (DBT) region since local crack-tip instability may trigger catastrophic structural failure under stresses well below the material yield stress.

Early procedures (e.g., ASME reference curve) adopted a deterministic lower bound based on the available plane strain fracture toughness database (i.e., ASME K_{IC} and K_{IR} reference curves, see (Riccardella and Yukawa, 1991; Wallin, 1999) for further details) and, therefore, do not consider neither the failure probability nor the statistical scatter coupled with fracture toughness measurements in the DBT region. Recent developments based on statistical concepts led to a more rational approach, often known as the Master Curve approach (Wallin, 1991, 1993; Merkle *et al.*, 1998; Wallin, 2002; McCabe *et al.*, 2005) and standardized in the form of ASTM E1921 (2020), to define an indexing (or reference) temperature, T_0, related to the median fracture toughness of K_{Jc}-values experimentally measured from standard $1T$ fracture specimens. Previous studies (Joyce and Tregoning, 2001; McCabe *et al.*, 2005) have shown that the Master Curve methodology is highly effective in describing the dependence of fracture toughness on temperature for a wide range of pressure vessel steels, irradiated steels and other structural ferritic steels with a yield strength in the range of $275\ MPa - 825\ MPa$. Recent studies have conducted exploratory analyzes in many different types of steel, including ultra-high strength steels (Neimitz *et al.*, 2012; Wallin *et al.*, 2015) and duplex stainless steel (Faccoli and Roberti, 2013). However, while the Master Curve approach (Merkle *et al.*, 1998; McCabe *et al.*, 2005) and ASTM E1921 (ASTM E1921, 2020) standard represent a significant advancement in fracture toughness characterization for ferritic steels in the lower ductile-to-brittle transition (DBT) region, there is very limited work that supports the applicability of the methodology

and, further, the accuracy of T_0 estimates to high strength martensitic steels (usually above 1000 MPa of yield stress) employed in structural and wear applications involving harsh environments working.

Motivated by these observations, this work addresses an experimental investigation of the brittle fracture behavior for a high strength martensitic steel using conventional three-point, bend, SE(B), specimens. The purpose of this work is to assess the applicability of the Master Curve methodology in providing a reliable estimate of the reference temperature (T_0) derived from fracture toughness data sets measured in the ductile-to-brittle transition region (DBT) of a direct-quenched low alloy martensitic steel. Even though the toughness-temperature behavior and scatter were shown to deviate from the ASTM E1921 predictions, the use of Master Curve in its standard formulation still provides a good description of the fracture toughness dependence with temperature for the tested material.

2. OVERVIEW OF THE MASTER CURVE APPROACH

Based on the seminal work of Landes and Shaffer (1980), which have clearly revealed the statistical nature of cleavage fracture for steels that exhibit a fracture mode transition, Wallin (1984) showed that the brittle fracture probability based upon experimentally measured fracture toughness values in the DBT, including lower-shelf region, is well described by a three-parameter Weibull cumulative distribution function for K_{J_c}-values given by

$$F\left(K_{J_c}\right) = 1 - exp\left[-\frac{B_{(nT)}}{B_{(1T)}}\left(\frac{K_{J_c} - K_{min}}{K_0 - K_{min}}\right)^{\alpha}\right] \tag{1}$$

in which $F(K_{J_c})$ is the probability of failure at or before K_{J_c} for an arbitrarily selected specimen taken from a specimen set, α defines the Weibull modulus (which characterizes the scatter in test data and is defined equals to 4 (Wallin, 1984; ASTM E1921, 2020)), K_0 is the characteristic toughness (also known as scale parameter, which approximately describes the mean value, K_{mean}, of the test data given by $K_{mean} = K_0\Gamma(1 + \alpha^{-1})$ with Γ defining the Gamma function (Mann *et al.*, 1974) and K_{min} denotes the threshold K-value of 20 $MPa\sqrt{m}$ as given by ASTM E1921 (Wallin, 1984; ASTM E1921, 2020). The term $B_{(nT)}/B_{(1T)}$ derives from the weakest link mechanism (or statistical weakest-link theory) (Wallin, 1985) used to adjust specimen size effects on K_{J_c}-values measured in the transition range between lower shelf and upper shelf fracture toughness of similar fracture specimens with different thicknesses in form of the Eq. 3 presented next. Moreover, as regards the Eq. (1), the K_{J_c}-values are obtained from J-integral at instability point (J_c) using the standard relationship between K and J (Rice, 1968; Hutchinson, 1983) expressed by:

$$K_{J_c} = \sqrt{\frac{J_c E}{(1-\nu^2)}} \tag{2}$$

where K_{J_c} is the fracture toughness (expressed in $MPa\sqrt{m}$ units) converted from J-integral measured at instability point (i.e., J_c value expressed in kJ/m^2 units), E is the elastic (longitudinal) modulus and ν is Poisson's ratio.

Since the Weibull distribution describes a probabilistic behavior of fracture obeying the weakest-link theory (Landes and Shaffer, 1980; Wallin, 1985), it is also possible to consider the specimen size effects on individual K_{J_c} values from the following expression:

$$K_{J_{c(1T)}} = K_{min} + \left[K_{J_{c(nT)}} - K_{min}\right]\left[\frac{B_{(nT)}}{B_{(1T)}}\right]^{(1/4)} \tag{3}$$

in which $K_{J_{c(1T)}}$ represents the size-adjusted individual K_{J_c} value, $K_{J_{c(nT)}}$ corresponds to the K_{J_c} value obtained from a specimen whose gross thickness $B_{(nT)}$ (i.e., side grooves shall be ignored) is different from $1T$ standard thickness, $B_{(1T)}$. Further, all toughness values must satisfy the maximum K_{J_c} capacity for the specimen, $K_{J_c-limit}$, which is given by ASTM E1921 (2020) as

$$K_{J_c-limit} = \sqrt{\frac{E b_o \sigma_{ys}}{(1-\nu^2)}} \tag{4}$$

where $b_o = W - a_o$ and σ_{ys} represent the uncracked ligament depth and the material yield stress. Particular attention shall be taken when using Eq. (4) once both elastic (longitudinal) modulus and yield stress shall be associated therewith test temperature. The K_{J_c} values above the validity criteria must be marked as censored data in the procedure to estimate the reference temperature, T_0, either from single temperature analysis or multi-temperature analysis. These issues will be taken up in the next sections.

Once the T_0 value is determined, the complete fracture toughness characterization over the transition range can be accurately described by the following general expression:

$$K_{J_c(0.XX)} = K_{min} + \left\{\frac{(A - K_{min})}{[\ln(2)]^{\left(\frac{1}{4}\right)}} + \frac{(100 - A)}{[\ln(2)]^{\left(\frac{1}{4}\right)}} exp\left[C\left(T - T_0\right)\right]\right\}\left[\frac{B_{(1T)}}{B_{(nT)}}\right]^{\left(\frac{1}{4}\right)}\left[\ln\left(\frac{1}{1-0.XX}\right)\right]^{\left(\frac{1}{4}\right)} \tag{5}$$

in which $0.XX$ represents the cumulative probability level (a value established between 0 and 1), $K_{J_c(0.XX)}$ is the associated fracture toughness (where a level of $0.XX = 0.50$ defines the median fracture toughness - $K_{J_c(med)}$), T_0 defines the temperature at which $K_{J_c(med)}$ for a $25.4\ mm$ $(1T)$ thick specimen is $100\ MPa\sqrt{m}$, and A and C are the fitting coefficients of the reference fracture toughness curve, more commonly known as master curve (Wallin, 1991; Merkle *et al.*, 1998; Wallin, 2002; McCabe *et al.*, 2005). From an extensive fracture toughness database of reactor pressure vessel steels, Wallin (1991) showed that the best coefficients to describe the dependence of $K_{J_c(med)}$ (corresponding to a fracture specimen with $25.4\ mm$ thickness) on temperature were provided by $A = 30$ and $C = 0.019$. Therefore, once the reference temperature T_0 is known, the temperature dependence of the median fracture toughness in the DBT region can be estimated for different failure probability levels and specimen thicknesses. The next sections discuss the different methods used to estimate the T_0 value.

2.1 Single Temperature Method

For the fracture toughness tests conducted at a single temperature, the complete fracture toughness characterization within the transition region requires the characteristic fracture toughness determination, K_0, (also known as scale parameter of the 3P Weibull distribution - see Eq.(1)). Following a standard maximum likelihood estimation procedure (Mann *et al.*, 1974; ASTM E1921, 2020), the scale parameter, K_0, corresponding to the 63.2% cumulative failure probability in previous Eq. (1), is given by

$$K_0 = \left[\sum_{i=1}^{N} \frac{\left(K_{J_c(i)} - 20\right)^4}{r}\right]^{\left(\frac{1}{4}\right)} + 20 \qquad MPa\sqrt{m} \tag{6}$$

in which $K_{J_c(i)}$ denotes the individual $K_{J_c(1T)}$ toughness data, N the total number of tested specimens and r represents the number of valid tests ($r = N - c$, where c is the number of invalid or censored toughness data points), which are considered as uncensored data in the present context - see ASTM E1921 (2020). According to Eq. (1) previously shown, the characteristic fracture toughness can be associated with a specific fracture toughness, $K_{J_c(0.XX)}$, by

$$K_{J_c(0.XX)} = \left\{\left[\ln\left(\frac{1}{1-0.XX}\right)\frac{25.4}{B_{(nT)}}\right]^{\left(\frac{1}{4}\right)}(K_0 - 20)\right\} + 20 \tag{7}$$

The single temperature approach determines the reference temperature, T_0, from evaluation of the median toughness, $K_{J_c(0.5)}$, at the tested temperature given by

$$K_{J_c(med)} = \left\{[\ln(2)]^{\frac{1}{4}}\left[\frac{25.4}{B_{(nT)}}\right]^{\left(\frac{1}{4}\right)}(K_0 - 20)\right\} + 20 \tag{8}$$

Finally, the reference temperature is obtained by using the $K_{J_c(med)}$ value determined for the data set at the test temperature by using the following equation:

$$T_0 = T - \left(\frac{1}{0.019}\right)\ln\left[\frac{K_{J_c(med)} - 30}{70}\right] \qquad {}^{\circ}C \tag{9}$$

where it is understood that Eq. (9) derives directly from Eq. (5) after some rearrangements.

2.2 Multitemperature Method

While the single temperature procedure is based on a straightforward analysis, important practical situations, such as the need to use small specimens (thickness < $1T$) due to severe limitations on material availability, may require tests at several different temperatures. Thus, when fracture toughness data measured at different DBT region temperatures are available, a multi-temperature maximum likelihood approach (Merkle *et al.*, 1998; McCabe *et al.*, 2005; ASTM E1921, 2020) can be used to evaluate the reference temperature T_0. Here, the T_0 value can be evaluated by an iterative solution obeying the following equality:

$$\sum_{i=1}^{N} \frac{\delta_i exp\left[C\left(T_i - T_0\right)\right]}{\frac{(A-20)}{\ln(2)^{\frac{1}{4}}} + \frac{(100-A)}{\ln(2)^{\frac{1}{4}}} exp\left[C\left(T_i - T_0\right)\right]} - \sum_{i=1}^{N} \frac{\left[K_{J_{c(i)}} - 20\right]^4 exp\left[C\left(T_i - T_0\right)\right]}{\left\{\frac{(A-20)}{\ln(2)^{\frac{1}{4}}} + \frac{(100-A)}{\ln(2)^{\frac{1}{4}}} exp\left[C\left(T_i - T_0\right)\right]\right\}^5} = 0 \tag{10}$$

where the Kronecker delta (δ_i) is 0 (for censored K_{J_c} data), or 1 (for valid K_{J_c} data). Regarding the censoring criteria established by the E1921 standard, the K_{J_c} values can be censored either by exceeding the limit deformation [i.e., $M_o < 30$, where $M_o = (Eb_o\sigma_{ys})/{K_{J_c}}^2$] or by presenting a large amount of ductile tearing which precedes the brittle fracture [i.e., slow stable crack growth that exceeds the smaller of either $0.05(W - a_o)$ or $1\ mm$].

3. EXPERIMENTAL DETAILS AND MATERIAL PROPERTIES

The material utilized in this study is a high-strength martensitic steel supplied as a hot rolled plate with a nominal thickness of $31.5\ mm$. This steel is hot rolled through CLC accelerated cooling (Continuous On-Line Control process, a sort of Thermo-Mechanical Control Process) followed by direct quenching. Its main characteristic is the high hardness which makes it suitable for service with high mechanical wear, being commonly applied in excavator components, off-road truck beds, shovels of wheel loaders, screens, crushers, channel linings, ore rail car, blast furnace components and industrial ventilators. Table 1 lists the chemical composition for the tested material which contains low carbon content (of the order of 0.25 weight percent), a moderately high manganese content (around 1.4 Mn), and small additions of boron which contribute to further increase hardenability.

Table 1: Chemical composition of tested martensitic steel ($\%$ weight).
Measured by atomic emission spectroscopy (AES).

C	**Mn**	**P**	**S**	**Nb**	**V**	**Ti**	**Cr**	**Ni**	**Mo**	**B**	**Ceq**
0.22	1.36	0.017	0.003	0.029	0.003	0.033	0.025	0.02	0.02	0.0010	0.50

Metallographic examination of an etched surface of the tested steel displayed in Fig. 1 revealed a predominantly lath martensite microstructure. These laths (i.e., long and thin plates) form side by side and are aligned parallel to one another which is typical for alloys containing less than approximately 0.6 wt$\%$ C (Campbell, 2012).

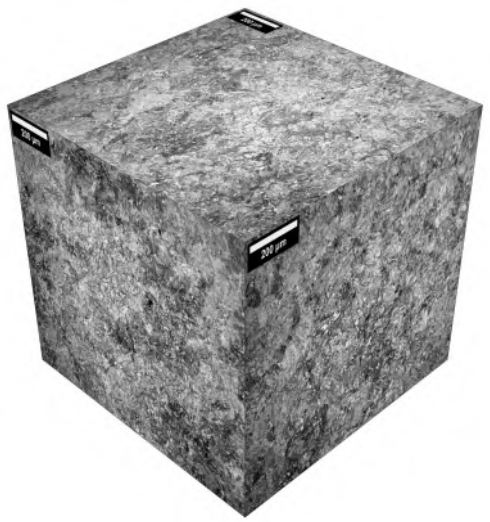

Figure 1: 3D view of the microstructure for the tested high-strength martensitic steel (Etching: Nital 2%. Magnification: 100x.

The tensile tests were conducted on three specimens at room temperature ($\sim 20\ ^oC$) providing a $1229\ MPa$ yield stress and $1371\ MPa$ tensile strength which far exceeds the upper limit of the yield stress range ($\sigma_{ys} \leq 825\ MPa$) allowable by the master curve approach. Furthermore, observe that the σ_{uts}/σ_{ys}-ratio of 1.1 evidence a remarkably low work-hardening behavior. For reference, an improved estimate for the hardening exponent given by *Annex F* of API RP-579-1 / ASME FFS-1 (2016) provides the strain hardening exponent at room temperature as $n = 20$, sharply contrasting the high hardening behavior ($n = 3 \sim 5$) (Savioli and Ruggieri, 2015) commonly presented by steels used in the Master Curve approach. Fig. 2a provides the individual engineering stress-strain curves for the high-strength martensitic steel at room temperature.

Since fracture tests are conducted in different DBT region temperatures (see further details next), the estimates for yield stress at each test temperature are provided by ASTM E1921 (2020) expression in the form:

$$\sigma_{ys}^{T-test} = \sigma_{ys}^{RT} + \frac{10^5}{491 + 1.8T} - 189 \qquad (MPa) \tag{11}$$

where σ_{ys}^{T-test} and σ_{ys}^{RT} define the material yield stress at the test temperature and at the room temperature in MPa, and T is the test temperature in $^\circ C$. Other mechanical properties for this material include Poisson's ratio, $\nu = 0.3$ and Young's modulus also estimated at the test temperature from the expression provided by ASTM E1921 (2020) as

$$E = 204 - \frac{T}{16} \qquad (GPa) \tag{12}$$

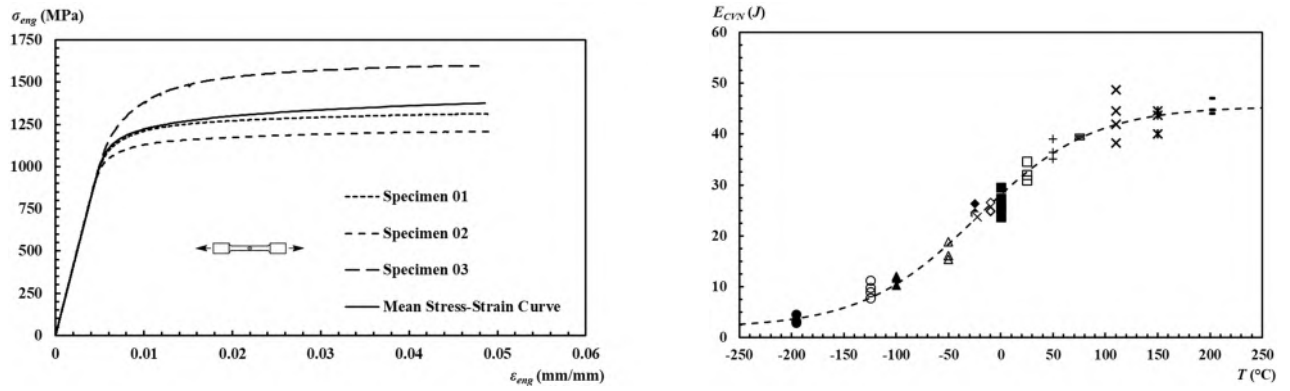

(a) (b)

Figure 2: (a) Engineering stress-strain curves for the tested high-strength martensitic steel at room temperature and (b) Charpy-V impact energy (T-L orientation) versus temperature for the tested high-strength martensitic steel.

The yield stress (σ_{ys}^{T-test}) and Young's modulus estimated values are used to determine the crack tip deformation relative to the remaining ligament ($b_o = W - a_o$) and, thus, the specimen measuring capacity at test temperature necessary to perform the statistical analysis of the measured J_c-values and their corresponding K_{J_c}-values.

A set of 44 standard three-point impact Charpy specimens (10 x 10 x 55 mm) with a 45° V-notch of 2 mm depth and 0.25 mm radius was extracted from the mid-thickness in the T-L plate orientation. This set was tested in a 406 J full scale Tinius-Olsen pendulum machine following the requirements of ASTM E23 (2018) standard. The Charpy impact tests were carried out using thirteen different temperatures, namely: -196 $°C$, -125 $°C$, -100 $°C$, -50 $°C$, -25 $°C$, -10 $°C$, 0 $°C$, 25 $°C$, 50 $°C$, 75 $°C$, 110 $°C$, 150 $°C$ and 200 $°C$. Figure 2b shows the measured toughness-temperature properties for the material in terms of conventional Charpy V-Notch impact energy (T-L orientation). In this plot, the symbols represent the experimentally measured Charpy energy, and the dashed line defines a hyperbolic tangent curve fitting proposed earlier by Oldfield (1979) and adopted later by EricksonKirk *et al.* (2008) with the lower shelf value set to a constant value of 2 $Joules$ for the experimental data set in the form:

$$CVE = 24 + 22\tanh\left(\frac{T+23}{110}\right) \qquad °C, J \tag{13}$$

where CVE denotes the Charpy V-notch energy expressed in J, T is the test temperature in degrees Celsius. Using the $tanh$-fitting expression, the Charpy transition temperatures corresponding to 28 J and 41 J energy yield approximately $T_{28J} = -0.6$ $°C$ and $T_{41J} = 96.7$ $°C$.

4. TEMPERATURE EFFECTS ON THE FRACTURE TOUGHNESS BEHAVIOR

To investigate the temperature effects on brittle fracture behavior of the martensitic steel employed in this study, a series of toughness tests was performed at different temperatures of the ductile-to-brittle transition region. Following the requirements of ASTM E1921 (2020), fracture toughness tests under displacement control were conducted on conventional, plane-sided three-point bend fracture specimens in the T-L orientation. Similar to Charpy specimens, all fracture SE(B) specimens were extracted from the mid-thickness of the plate. The SE(B) specimens have standard $1T$ thickness ($B = 25.4mm$) with a fixed overall geometry defined by a cross-section $W/B = 2$, a crack length (a) to width (W) ratio of $a/W = 0.5$, and load span (S) given by $S/W = 4$ ratio.

The fracture mechanics tests of this specimen configuration were performed at -20 to 70 $°C$ range temperature to measure the values of the J-integral at instability point, here defined as J_c - as shown previously in Fig. 2b, this range temperature corresponds to the middle to upper transition region for the tested high-strength martensitic steel.

Thus, to illustrate the temperature effects on the fracture behavior, Fig. 3a displays typical load-displacement curves (as described by CMOD) measured from testing the deeply cracked SE(B) specimens with $a/W = 0.5$ at different temperatures. In these plots, each of these curves corresponds to a specimen for which the measured J_c-value is similar to the characteristic toughness, J_0, of the corresponding statistical distribution of measured J_c-values − see Section 5next for further details.

Based on Figure 3a, the temperature effects on load-displacement curve behavior are clearly evident. As we can see, the material behaves in a fully brittle manner at low temperatures, including at room temperature, albeit this range temperature is representative of the DBT middle transition region as shown by the Charpy V-Notch impact energy transition curve set out in Figure 2b. Conversely, the P-CMOD curves related to tests conducted between 50 and 70 $°C$, which range corresponds to the upper transition region in Fig. 2b, show an elastic-plastic behavior prior to final instability. This

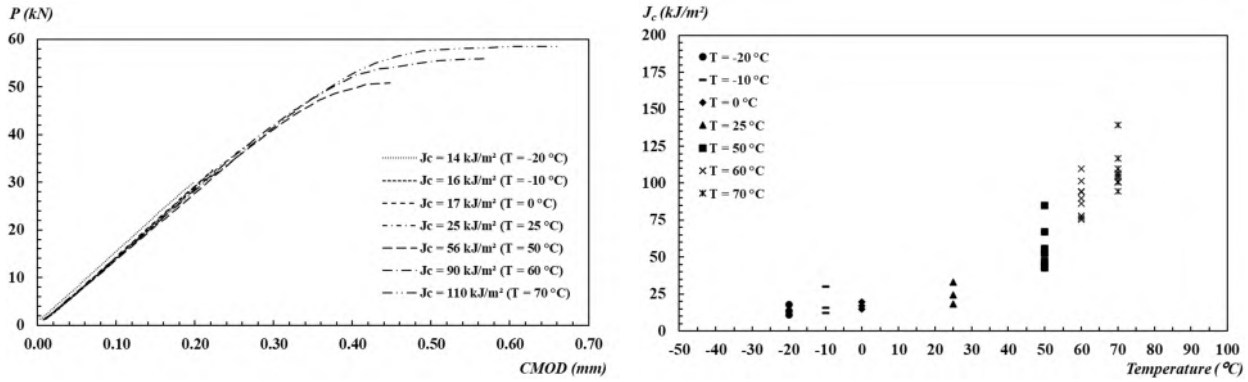

(a) (b)

Figure 3: (a) Representative load-displacement response for the tested martensitic steel corresponding to different temperatures and (b) Description of the dependence of fracture toughness on temperature for a wide temperature range in the DBT region.

behavior may imply in fracture toughness measurements temperature-dependent and, at the same time, a test temperature closest to the reference temperature.

To facilitate description of the temperature dependence of fracture toughness, all toughness data are displayed in a plot that correlates the measured J_c-values with the test temperature as shown in Figure 3b. Here, the trends are clear as temperature strongly affects the fracture behavior for the martensitic steel used in this study. To the extent that temperature increases, both the upper and lower bound of fracture toughness also increase. According to Fig. 3b, it is noticeable the exponential behavior of fracture toughness as test temperature increases providing strong support to the master curve analysis for the tested material. Further, observe that the toughness data scatter is higher for the test temperature range 50 to $70\ ^{\circ}C$ which vindicates a particular emphasis for these data. Thus, the following section addresses the fracture toughness distributions in terms of a three-parameter Weibull distribution only for this specific test temperature range which in turn correspond to the upper transition region of the Charpy energy curve.

Even though the Charpy V-Notch impact energy transition curve (see Fig. 2b) has shown that the -20 to $25\ ^{\circ}C$ temperature range corresponds to the mid-transition region for the martensitic steel used in the present study, the response in terms of fracture mechanism resembles pure cleavage dominated only by propagation step that typically occurs in ferritic steels which operate at lower shelf temperatures (Anderson and Stienstra, 1989; Ruggieri *et al.*, 1995; Merkle *et al.*, 1998).

Considering these observations, after some preliminary fracture tests to emphasize the ductile-to-brittle transition region, three different test temperatures were chosen as proper values for the master curve purpose, namely: $50\ ^{\circ}C$, $60\ ^{\circ}C$, and $70\ ^{\circ}C$ which correspond to the upper transition region (i.e., upper portion of the DBT region). Regarding the $50\ ^{\circ}C$ to $70\ ^{\circ}C$ range, nine specimens were used for each test temperature aiming for a suitable quantity of specimens to estimate a reliable reference temperature.

5. FRACTURE TOUGHNESS DISTRIBUTION

Evaluation of plane-strain fracture toughness values, here characterized in terms of the elastic-plastic critical J-integral value corresponding to brittle fracture, J_c, follows from determining the plastic area under the experimentally measured load-CMOD curve and then using the estimation procedure based on η-factors outlined in ASTM E1820 (2020) for each test specimen and test temperature. Since none of the tested specimens at -20 to $70\ ^{\circ}C$ showed subcritical crack growth prior to unstable fracture neither a deformation limit lower than the assigned value of 30 as per ASTM E1921 (2020), all data is treated as non-censored toughness values as discussed next.

The (rank-ordered) cumulative probability distributions of the measured J_c-values for fracture specimens tested at temperature range 50 to $70\ ^{\circ}C$ are displayed in Figure 4. The solid symbols in the plots indicate the experimental fracture toughness data for the specimens tested (as already observed, all data points displayed in Fig. 4 are valid results). The cumulative probability, $F(J_c)$, is derived by simply ranking the J_c-values in ascending order and using the median rank position defined in terms of $F(J_{c,k}) = (k - 0.3)/(N + 0.4)$, where k denotes the rank number and N defines the total number of experimental toughness values (Mann *et al.*, 1974). The fitting curves (represented by the dashed lines) to the rank-ordered experimental data shown in Fig. 4 describe the three-parameter Weibull distribution (Mann *et al.*, 1974) for J_c-values given by:

$$F\left(J_c\right) = 1 - exp\left[-\frac{B_{(nT)}}{B_{(1T)}}\left(\frac{J_c - J_{min}}{J_0 - J_{min}}\right)^{\alpha}\right] \tag{14}$$

in which α defines the Weibull modulus (which characterizes the scatter in test data) and is allotted a value of 2, J_0 is the characteristic toughness (which corresponds to the 63.2% cumulative failure probability) and J_{min} denotes the threshold J-value corresponding to a K_{min} of 20 $MPa\sqrt{m}$ as given by ASTM E1921 (2020).

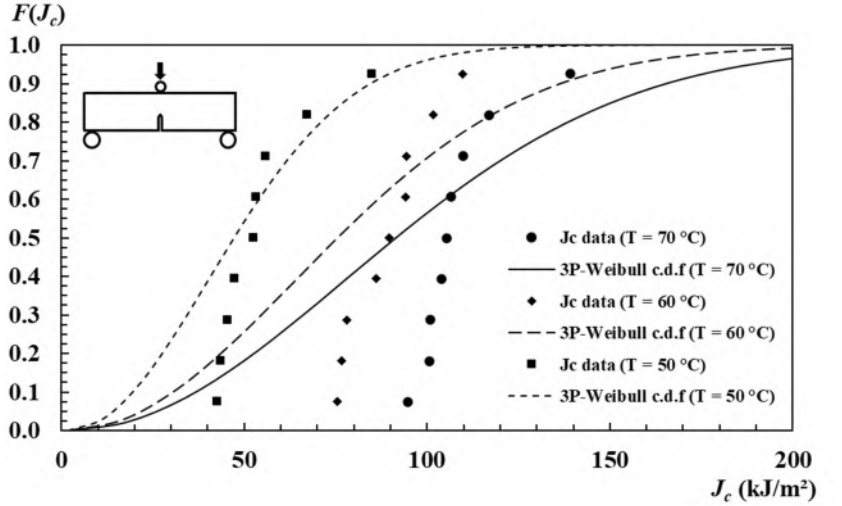

Figure 4: Cumulative Weibull distribution of experimentally measured J_c-values of the high-strength martensitic steel for standard SE(B) fracture specimens tested at 50, 60 and 70 $^\circ C$.

The fracture toughness distributions displayed in Fig. 4 reveal that the martensitic steel used in this study is highly sensitive to small temperature changes in the upper transition region. Here, it is observed that an increase from 50 $^\circ C$ to 60 $^\circ C$ considerably shifts the J_c-distribution to the right. However, this shift is smaller for higher temperatures suggesting that temperatures greater than 70 $^\circ C$ may introduce ductile tearing effects prior to brittle fracture. Further, observe that the upper bound of the rank-ordered J_c-values fits relatively well on the three-parameter Weibull Cumulative Distribution for the selected test temperature range. Conversely, the lower bound is not well adjusted, mainly for the J_c-values measured at 60 and 70 $^\circ C$.

Table 2: Maximum likelihood estimates of the characteristic toughness, $\hat{J}_0$, for the distributions of the J_c-values measured at 50, 60 and 70 $^\circ C$

T ($^\circ C$)	$\hat{J}_0$ ($\alpha_J = 2$)	$\hat{\alpha}_J$	$\hat{J}_0$ ($\hat{\alpha}_J$)	$\Delta\hat{J}_0$
50	56.7	3.5	64.6	13.9
60	90.3	7.9	92.9	2.8
70	109.5	8.3	113.0	3.2

The data analysis showed in Tab. 2 reveals that this behavior is directly related to the markedly low scatter presented by the measured J_c-values for the martensitic steel used in this study. Here, it is observed a narrower scatter for the J_c-values measured at 60 and 70 $^\circ C$, while the J_c-values measured at 50 $^\circ C$ show a relatively higher scatter according to the Weibull modulus values ($\hat{\alpha}_J$) estimated by the maximum likelihood method (Rinne, 2008). In turn, this lower scatter is somewhat related to the microstructural features, once the material used in this study is a direct-quenched high-strength steel which sharply contrasts with the pressure vessel ferritic steels and structural ferritic steels typically used in the master curve approach. For these steels, the scatter in the transition range is effectively controlled by the cleavage fracture initiation process in the ferrite phase, which can be different for the case of the martensitic phase of the steel used in this study. However, perhaps the most important observation is the estimated characteristic toughness ($\hat{J}_0$) is almost insensitive to the Weibull modulus (α) and, thus, to the toughness scatter, as can be shown in Table 2.

6. EVALUATION OF THE REFERENCE TEMPERATURE, T_0

Following the development provided in ASTM E1921 (2020), the reference temperature for the tested material is evaluated either from the single and multi-temperature analysis.

Figure 5 provides the variation of $K_{Jc(med)}$ with temperature for the tested high-strength martensitic steel at different temperatures. Regarding the data scatter description by the median curve relying on single temperature analysis, which represents 50 % cumulative failure probability, note that the master curve passes through the bottom of all data sets. This behavior suggests that the fracture toughness dependence with temperature is sharper than the expected variation provided by the standard master curve, as the temperature increases. Further, observe that all the data falls within tolerance bounds.

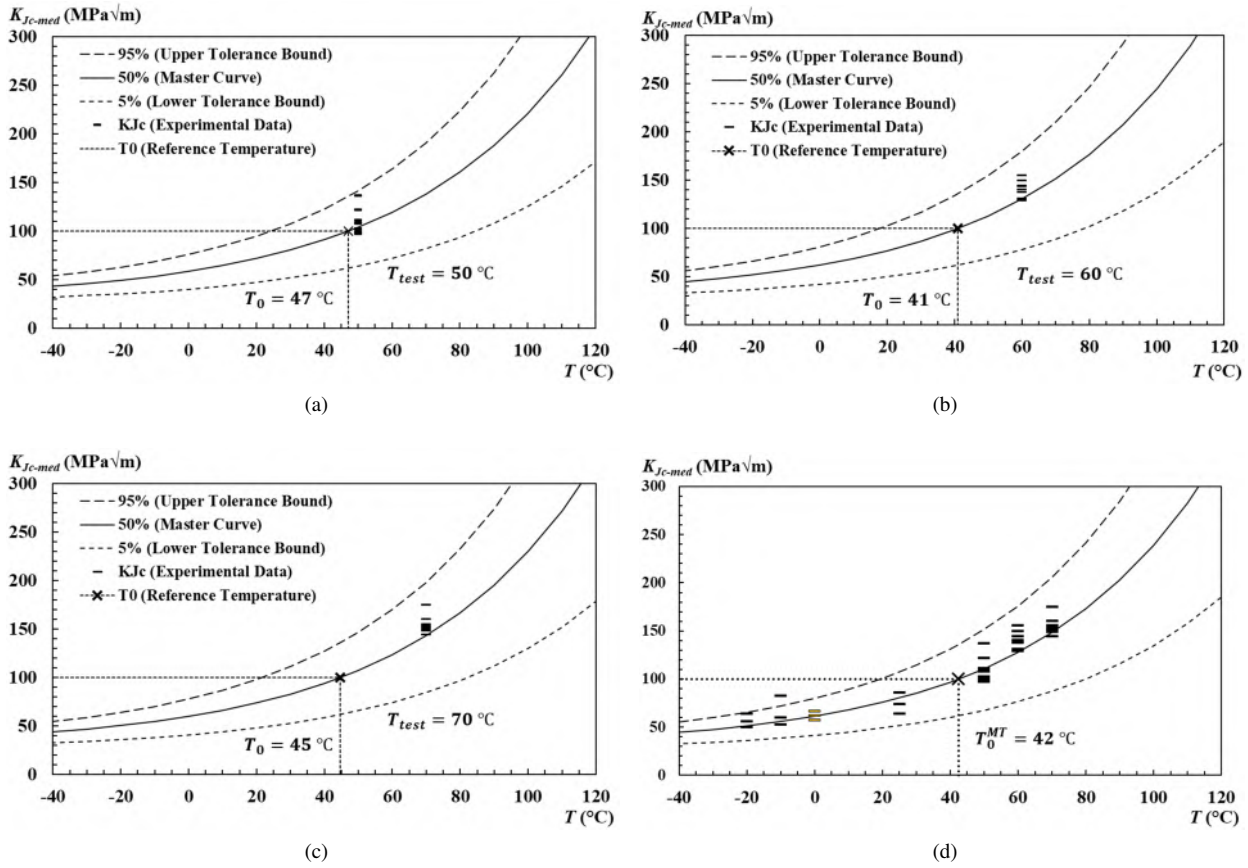

Figure 5: Master curve for the tested high-strength martensitic steel including 5% and 95% confidence bounds based on cleavage fracture toughness values measured from standard $1T$ SE(B) specimens at (a) $50\ ^{\circ}C$; (b) $60\ ^{\circ}C$, (c) $70\ ^{\circ}C$ and (d) on -20 to $70\ ^{\circ}C$ temperature range.

Regarding the reference temperature, it is possible to note all T_0 estimates (T_0^{est}) are valid since the difference between test temperature (T) and estimated reference temperature T_0^{est} is less than $50\ ^{\circ}C$.

While testing is allowed at any temperature within $T_0 \pm 50\ ^{\circ}C$, the most accurate estimates of T_0 (T_0^{est}) are obtained by testing as close to material reference temperature as possible. Special attention is given to the master curve obtained from tests conducted at $50\ ^{\circ}C$ (see Fig. 5a). Here, the difference between the test and reference temperature is only $3\ ^{\circ}C$, which provides a highly accurate reference temperature estimation. Regarding the master curve obtained from tests conducted at 60 and $70\ ^{\circ}C$, see Figures 5b and 5c, despite the difference is relatively higher, the T_0-values estimated at both temperatures are near the T_0 estimated at $50\ ^{\circ}C$. These values provide strong evidence that the material T_0 estimated according to ASTM E1921 (2020) is within 40 and $50\ ^{\circ}C$ range.

In order to provide a more accurate estimation of the measured T_0 value, Fig. 5d provides the master curve based on a multi-temperature approach in which the evaluation procedure encompasses a larger data set of K_{Jc} values corresponding to a wide range of the DBT region. Observe that the T_0-value evaluated from K_{Jc}-values measured at -20 to $70\ ^{\circ}C$ is also within 40 and $50\ ^{\circ}C$ range which corroborates the accuracy of the other T_0 values. Similar to the single temperature master curves, the data scatter description by the median curve derived from the multi-temperature analysis also intercepts the bottom of almost all data sets. Again, this behavior shows that the dependence of fracture toughness on temperature is more pronounced than the standard master curve prediction, suggesting new coefficients for the master curve to a better description of fracture toughness dependence with temperature for the martensitic steel used in this study.

7. CONCLUDING REMARKS

This work presented an exploratory application to determine the reference temperature, T_0, of a high-strength martensitic steel based on the standard Master Curve approach. The purpose of this work is to assess the applicability of the Master Curve methodology in providing a reliable estimate of the reference temperature (T_0) derived from fracture toughness data sets measured at different temperatures over the ductile-to-brittle transition region (DBT) of a direct-quenched low alloy martensitic steel.

From the fracture toughness tests conducted at the DBT region, it is shown that the high-strength martensitic steel

exhibited a smaller scatter than predicted by the standard master curve approach. However, the experimental results clearly show a relatively strong effect of temperature on measured J_c-values and corresponding K_{Jc}-values for the tested material providing strong support for using the master curve approach. Further, even though the data scatter and fracture toughness temperature dependence deviate somewhat from the standard median curve, the master curve approach still provides an accurate reference temperature and a good description of the fracture toughness dependence with temperature for the tested high-strength martensitic steel.

8. ACKNOWLEDGMENTS

This investigation is supported by Fundação de Amparo à Pesquisa do Estado de São Paulo (FAPESP) through research grant 2016/26024-1. The first author (VMCG) would like to acknowledge the financial support from Coordenção de Aperfeiçoamento de Pessoal de Nível Superior (CAPES). The work of CR is also supported by the Brazilian Council for Scientific and Technological Development (CNPq) through grant 306193/2013-2.

9. REFERENCES

Anderson, T. and Stienstra, D., 1989. "A model to predict the sources and magnitude of scatter in toughness data in the transition region". *Journal of Testing and Evaluation*, Vol. 17, No. 1, pp. 46–53.

API RP-579-1 / ASME FFS-1, 2016. "Recommended practice for fitness-for-service".

ASTM E1820, 2020. "Standard test method for measurement of fracture toughness, ASTM E1820-20".

ASTM E1921, 2020. "Standard test method for determination of reference temperature, T_0, for ferritic steels in the transition range, ASTM E1921-20".

ASTM E23, 2018. "Standard test method for notched bar impact testing of metallic materials, ASTM E23-18".

BS 7910, 2019. "Guide to methods for assessing the acceptability of flaws in metallic structures, BS 7910".

Campbell, F.C., 2012. *Phase Diagrams: Understanding the Basics*, ASM International, chapter 15: Nonequilibrium Reactions: Martensitic and Bainitic Structures, pp. 303–338.

ErickssonKirk, M.T., Shaikh, A. and ErickssonKirk, M.A., 2008. "Insights and observations arising from curve-fitting the Charpy V-notch and tensile data contained within the United States Light Water reactor surveillance database". In *ASME PVP 2008 Pressure Vessel and Piping Division Conference* . American Society of Mechanical Engineers, Chicago, IL.

Faccoli, M. and Roberti, R., 2013. "Probabilistic fracture toughness of a duplex stainless steel in the transition range". *Engineering Fracture Mechanics*, Vol. 97, pp. 207–215.

Hutchinson, J.W., 1983. "Fundamentals of the phenomenological theory of nonlinear fracture mechanics". *Journal of Applied Mechanics*, Vol. 50, pp. 1042–1051.

Joyce, J.A. and Tregoning, R.L., 2001. "Development of the T_0 reference temperature from precracked charpy specimens". *Engineering Fracture Mechanics*, Vol. 68, pp. 861–894.

Landes, J. and Shaffer, D., 1980. "Statistical characterization of fracture in the transition region". In P.C. Paris, ed., *Fracture Mechanics: Proceedings of the Twelfth National Symposium on Fracture Mechanics*. American Society for Testing and Materials, West Conshohocken, PA, ASTM STP 700, pp. 368–382.

Mann, N.R., Schafer, R.E. and Singpurwalla, N.D., 1974. *Methods for Statistical Analysis of Reliability and Life Data*. Jonh Wiley & Sons, New York.

McCabe, D.E., Merkle, J.G. and Wallin, K., 2005. "An introduction to the development and use of the master curve method". ASTM Manual Series 10.1520/MNL52-EB, ASTM International.

Merkle, J., Wallin, K. and McCabe, D., 1998. *Technical basis for an ASTM standard on determining the reference temperature, T0, for ferritic steels in the transition range*. Number ORNL/TM-13631 in Oak Ridge National Laboratory Technical Report. U.S. Nuclear Regulatory Commission, United States. Project code: V7SU00063.

Neimitz, A., Dzioba, I. and Limnell, T., 2012. "Modified master curve of ultra high strength steel". *International Journal of Pressure Vessels and Piping*, Vol. 92, pp. 19–26.

Oldfield, W., 1979. "Fitting curves to toughness data". *Journal of Testing and Evaluation*, Vol. 7, No. 6, pp. 326–333.

Riccardella, P.C. and Yukawa, S., 1991. "Twenty years of fracture mechanics and flaw evaluation applications in the asme nuclear code". *Journal of Pressure Vessel Technology*, Vol. 113, No. 2, pp. 145–153.

Rice, J.R., 1968. "A path independent integral and the approximate analysis of strain concentration by notches and cracks". *Journal of Applied Mechanics*, Vol. 35, pp. 379–386.

Rinne, H., 2008. *The Weibull Distribution A Handbook - 1st Edition*. Chapman and Hall/CRC, New York, NY.

Ruggieri, C., Minami, F. and Toyoda, M., 1995. "A statistical approach for fracture of brittle materials based on the chain-of-bundles model". *Journal of Applied Mechanics*, Vol. 62, pp. 320–328.

Savioli, R.G. and Ruggieri, C., 2015. "Experimental study on the cleavage fracture behavior of an ASTM A285 Grade C pressure vessel steel". *ASME Journal of Pressure Vessel Technology*, Vol. 137, No. 2, pp. 1–7.

Wallin, K., 1984. "The scatter in K_{Ic} results". *Engineering Fracture Mechanics*, Vol. 19, pp. 1085–1093.

Wallin, K., 1985. "The size effect in K_{Ic} results". *Engineering Fracture Mechanics*, Vol. 22, No. 1, pp. 149–163.

Wallin, K., 1991. "Fracture toughness transition curve shape for ferritic structural steels". In S.H. S.H. Teoh and K.H. Lee, eds., *Joint FEFG/IICF International Conference on Fracture of Engineering Materials and Structures* . Singapore, pp. 83–88.

Wallin, K., 1993. "Irradiation damage effects on the fracture toughness transition curve shape for reactor pressure vessel steels". *International Journal of Pressure Vessel and Piping*, Vol. 55, pp. 61–79.

Wallin, K., 2002. "Master curve analysis of the Euro fracture toughness dataset". *Engineering Fracture Mechanics*, Vol. 69, pp. 451–481.

Wallin, K., 1999. "Re-evaluation of the ASME K_{IC} and K_{IR} fracture toughness reference curves". *Nuclear Engineering and Design*, Vol. 193, No. 3, pp. 317–326.

Wallin, K., Pallaspuro, S., Valkonen, I., Karjalainen-Roikonen, P. and Suikkanen, P., 2015. "Fracture properties of high performance steels and their welds". *Engineering Fracture Mechanics*, Vol. 135, pp. 219–231.

10. RESPONSIBILITY NOTICE

The following text, properly adapted to the number of authors, must be included in the last section of the paper: The author(s) is (are) solely responsible for the printed material included in this paper.